Published in final edited form as:

Virology. 2013 November ; 446(1-2): 230–237. doi:10.1016/j.virol.2013.07.038.

Development of a reverse genetics system to generate recombinant Marburg virus derived from a bat isolate☆

César G. Albariño[1], **Luke S. Uebelhoer**[1], **Joel P. Vincent**, **Marina L. Khristova**, **Ayan K. Chakrabarti**, **Anita McElroy**, **Stuart T. Nichol**, and **Jonathan S. Towner**[*]

Centers for Disease Control and Prevention, Atlanta, GA 30333, USA

Abstract

Recent investigations have shown the Egyptian fruit bat (*Rousettus aegyptiacus*) to be a natural reservoir for marburgviruses. To better understand the life cycle of these viruses in the natural host, a new reverse genetics system was developed for the reliable rescue of a Marburg virus (MARV) originally isolated directly from a *R. aegyptiacus* bat (371Bat). To develop this system, the exact terminal sequences were first determined by 5′ and 3′ RACE, followed by the cloning of viral proteins NP, VP35, VP30 and L into expression plasmids. Novel conditions were then developed to efficiently replicate virus mini-genomes followed by the construction of full-length genomic clones from which recombinant wild type and GFP-containing MARVs were rescued. Surprisingly, when these recombinant MARVs were propagated in primary human macrophages, a dramatic difference was found in their ability to grow and to elicit anti-viral cytokine responses.

Keywords

Filovirus; Marburgvirus; Marburg virus; Bat isolate; Minigenome; Recombinant; Full-length; GFP; Macrophages; Cytokines

Introduction

Marburgviruses (family *Filoviridae*) are the causative agents of large hemorrhagic fever outbreaks in sub-Saharan Africa with high case fatality. The genus *Marburgvirus* contains a single virus species that has two virus members, Marburg virus (MARV) and Ravn virus (RAVV). As members of the Order *Mononegavirales*, marburgviruses contain single-stranded RNA genomes of negative polarity and are approximately 19 kilobases in length. Marburgvirus genomes contain seven monocistronic genes, each consisting of transcription start/termination sequences, a 3′ and 5′ untranslated region, and a single open reading frame (ORF) (Sanchez et al., 2007). Relative to most other members of the *Mononegavirales*, marburgvirus intergenic regions are unusual in that they consist of short, variable nucleotide stretches, or contain highly conserved overlaps between the upstream

☆The findings and conclusions in this report are ours and do not necessarily represent the views of the Centers for Disease Control and Prevention.

[*]Corresponding author. jit8@cdc.gov (J.S. Towner).

[1]Equal contribution by authors.

gene transcription termination sequence and the corresponding downstream gene transcription start sequence (Feldmann et al., 1992).

For marburgviruses, the events that lead to virus spillover to humans are becoming better understood as mounting evidence shows that the Egyptian fruit bat (*Rousettus aegyptiacus*) is a natural reservoir (Amman et al., 2012; Swanepoel et al., 2007; Towner et al., 2009, 2007). This determination was based on epidemiologic linkage of many human outbreaks to large *R. aegyptiacus* populations and the repeated isolation of highly diverse marburgvirus lineages from bats caught at the site of known or suspected spillover events. Consistent with expectations for a virus that has co-evolved with its reservoir host, marburgviruses appear to cause little disease in *R. aegyptiacus* (Paweska et al., 2012; Towner et al., 2009), which contrasts the severe, often fatal disease found in human and non-human primates (NHPs).

Previous studies of MARV replication in experimentally infected *R. aegyptiacus* are difficult to interpret because the virus inoculum had been passaged 38 times in an interferon negative primate cell line (Vero cells) prior to its use (Paweska et al., 2012). Such extended replication in the absence of natural selective pressures will likely result in the accumulation of mutations that could reduce virus fitness if experimentally re-introduced into *R. aegyptiacus*. Therefore, as a first step to generate authentic tools for dissecting the viral molecular genetic determinants for future experimental infection studies of *R. aegyptiacus*, we developed an efficient and reproducible reverse genetics system to rescue a recombinant MARV possessing a genome RNA sequence based on an isolate (strain Uganda 371Bat2007, isolate 811277) originally obtained directly from a MARV-infected bat captured at Kitaka Cave in western Uganda (Towner et al., 2009). Both ‘wild type’ and GFP-containing viruses were rescued.

The sequence of 371Bat MARV differs from the closest human MARV isolate, 01Uga07, by 120 nucleotides across the genome. Presumably, if *R. aegyptiacus* are indeed the natural virus source from which humans become infected, then a low passaged (passage 2) bat-derived virus should likely replicate as well as a similarly passaged human-derived isolate when tested in human immunocompetent cells. To test this hypothesis, the growth of wild type (wt) and recombinant bat-derived MARVs were compared side-by-side with a similarly low passage human isolate in primary human macrophages. As predicted, the wild type bat- and human-derived viruses replicated to similar levels. However, the recombinant bat virus containing the GFP gene insertion in the virus genome was found to have diminished replication in macrophages and effected profound changes in the RNA expression levels of human host cell cytokine and chemokine genes. These data suggest that perturbations in natural virus transcriptional regulation may cause dramatic changes in the virus′s ability to carry out immune modulatory processes.

Results and discussion

Whole genome sequencing of the MARV isolate from 371Bat has been previously performed (Towner et al., 2009). The sequence (GenBank FJ750958) is <1% divergent from a virus isolated from an infected miner working in the same cave (01Uga2007, GenBank FJ750957), 7–8% divergent from some other well-characterized MARV lineage isolates

(including the Musoke strain), and >21% divergent from RAVN viruses (Fig. 1A). All sequences analyzed follow the basic filoviral genome organization of seven genes with intergenic regions and untranslated termini at both ends (Fig. 1B). Prior to attempting a cloning strategy, the terminal 5′ and 3′ UTRs of 371Bat virus were experimentally determined since these terminal 20 nucleotides were initially dictated by amplification primers during the original sequencing. Using rapid amplification of cDNA ends (RACE) it was found that two nucleotides near the 3′ end of the anti-genome differed from the original sequence. The first change consisted of an '*A*' residue at position 19105 of the original sequence that was clearly a '*T*' residue when experimentally determined (Fig. 1C, left box), while the second change was an incorrect insertion of an '*A*' residue at position 19114 in the original sequence (Fig. 1C, right box) indicating that the total genome length is in fact 19113 nucleotides and not 19114 nucleotides. The 5′ terminal nucleotide of the genomic sense RNA is now a '*C*'. We suspect that both differences were likely introduced by the primers used for generation of RT-PCR products from which the original sequence was determined.

Using the corrected sequence for the 371Bat virus, both mini- and full-length genome amplification systems were constructed. For the mini-genome system, RT-PCR was used to amplify the ORFs of 371Bat nucleoprotein (NP), viral protein (VP) 35, VP30, and polymerase (*L*), all of which were cloned using standard techniques into a pol II expression plasmid. As a negative control, an additional support plasmid was constructed that generated an inactive polymerase by substituting Ala residues for the highly conserved GDN motif found in the polymerase (Fig. 1D). For the GFP-containing mini-genome, the GFP sequence was cloned into a standard T7 transcription plasmid flanked by the 371Bat 3′ and 5′ UTRs in viral (genome) sense. BSR-T7/5 cells (Buchholz et al., 1999) stably expressing the T7 RNA polymerase were transfected with supporting and mini-genome plasmids, and monitored for GFP expression as an indicator of RNA transcription and replication. Cells expressed GFP as early as two days post-transfection, and reached maximum expression four days post-transfection (Fig. 2A). Co-transfection of NP, L, and VP35 supporting plasmids was sufficient to observe mini-genome replication (Fig. 2A), as has been previously reported (Muhlberger et al., 1998, 1999). Interestingly, addition of VP30 supporting plasmid increased the number of cells able to replicate the GFP mini-genome. As expected, the use of supporting polymerase plasmid containing the mutated GDN motif completely ablated GFP expression (Fig. 2A).

Although GFP expression was clearly detectable in BSR-T7/5 cells, the percentage of cells replicating mini-genomes was less than 30%. Additionally, the kinetics of this system was relatively slow (strongest GFP signal at 4d post-transfection), making it less than ideal for shorter-term experiments. To circumvent these problems, each support protein ORF was codon-optimized for rodent cell expression and cloned into the pol II expression vector. Co-transfection of these new plasmids (denoted by a "co" in Fig. 2) with the GFP mini-genome led to rapid GFP expression, with green cells visible by 24 h post-transfection (data not shown). By 48 h post-transfection, most BSR-T7/5 cells receiving all codon-optimized support plasmids expressed GFP (Fig. 2B). The largest single increase in GFP expression was brought about by the addition of the codon-optimized polymerase, although addition of all codon-optimized plasmids resulted in the greatest total number of cells expressing GFP and highest intensity of signal. Interestingly, codon-optimized NP or VP35 plasmids used

individually with non-optimized plasmids resulted in the poorest levels of GFP expression, even worse than the complete non-codon-optimized system, suggesting that the overexpression of NP or VP35 relative to the other replication proteins may somehow negatively affect replication. In contrast, the individual utilization of codon-optimized VP30 plasmid with non-optimized NP, VP35 and L resulted in similar GFP expression as the all non-codon-optimized system, confirming that VP30 expression does not have a dramatic positive or negative affect on mini-genome replication (Fig. 2B).

After conditions were determined for optimal mini-genome expression, a full-length recombinant clone based on the 371Bat virus genome sequence was constructed. This plasmid was initially built in viral complementary (antigenomic) sense (Fig. 3) as previously published data suggested that this orientation was the most efficient for viral rescue in Marburg and Ebola virus systems (Enterlein et al., 2006; Neumann et al., 2002; Volchkov et al., 2001). Three additional full-length 371Bat clones were built, each with the GFP gene inserted in one of the intergenic regions between NP-VP35, GP-VP40, or trailing the polymerase in the 3′ UTR. All four full-length clones were also constructed in the viral (genomic) sense. Initial attempts at rescue in BSR-T7/5 cells using all codon-optimized support plasmids were met with very limited success. Briefly, clarified supernatants or cell lysates from BSR-T7/5 collected at 3–7 days post-transfection were used to infect VeroE6 cells. Out of more than 100 separate attempts, only once was a recombinant virus rescued, and this virus contained GFP inserted in between NP and VP35 (data not shown).

During the course of these rescue experiments, it was noticed that the BSR-T7/5 cells would quickly become 100% confluent and undergo cell death despite carrying out the initial transfections when cells were <50% confluent. We therefore hypothesized that the rapid cell growth was resulting in the death of successfully transfected cells before detectable virus was produced. To overcome this problem, we performed similar transfections in the parental BHK-21 cell line which grow at a slower rate. Because BHK-21 cells do not constitutively express T7 RNA polymerase, the pC-T7 plasmid was additionally added to the transfection mix.

The rescue attempt in BHK-21 cells was successful, and the non-GFP recombinant ‘wild type’ virus (rMbg) was rescued for the first time in 4/22 wells of a single experiment (~20% efficiency, Fig. 3A). Moreover, the efficiency of virus rescue from rMbg-FL/GFP_{2849} was greatly increased in these cells, as evidenced by virus rescue in 21/24 wells of a single experiment (~90% efficiency, Fig. 3B). After performing a total of 12 rescue attempts in numerous independent experiments the results have remained remarkably consistent, with rescue of non-GFP viruses occurring with 20–30% efficiency and GFP-containing viruses (rMbg/GFP) at 70–95% efficiency. In spite of the initial success, no virus rescue was achieved when using full-length genomic-sense clones or antigenomic clones with GFP inserted between GP and VP40, or after the L gene 3′ UTR.

Once rescued, both viruses grew to similar titers in VeroE6 cells, with almost 100% of VeroE6 cells positive by IFA and/or GFP expression four days post-infection. Interestingly, rMbg/GFP seems to grow slightly faster in VeroE6 cell culture during the first three days of infection than either rMbg or wild type 371Bat virus (Fig. 3C). The faster growth phenotype

observed with rMbg/GFP virus in VeroE6 cells may partially explain why this virus is rescued with greater efficiency than the rMbg virus.

During early stages of marburgvirus infections of humans and NHPs, the primary sites of virus replication are thought to be monocytes, macrophages, and dendritic cells (Fritz et al., 2008; Geisbert and Jaax, 1998; Hensley et al., 2011). If bats are indeed the initial source of marburgviruses leading to human outbreaks, we reasoned that viruses derived directly from bats with little opportunity to accumulate cell culture adaptations should efficiently infect primary human macrophages. To test this hypothesis, we infected human CD14+ macrophages with a minimally passaged human isolate (01Uga07), wild type 371Bat virus, and both GFP and non-GFP recombinant 371Bat viruses, and compared viral growth. As expected, rMbg 371Bat virus and the 01Uga07 human isolate grew to similar levels, but interestingly rMbg/GFP virus grew to titers 1–2 logs less (Fig. 4B). This result was unexpected because rMbg and rMbg/GFP viruses grew to similar levels in VeroE6 cells (Fig. 3C), indicating that the insertion of an extra-cistronic gene between NP and VP35 did not affect the virus replication. To further explore the growth defect of the rMbg/GFP virus in human macrophages, mRNA levels of the genes up- and down-stream of the GFP insertion were measured by qRT-PCR. The infected cell data indicate that compared to rMbg virus, the rMbg/GFP virus showed a 50–80% decrease in the mRNA levels of the downstream VP35 and VP40 genes relative to the upstream NP mRNA (data not shown). This observation is consistent with the established paradigm for transcriptional polarity observed in single-strand negative sense RNA viruses and may indicate that, at least in macrophages, the GFP gene insertion results in lower levels of downstream replication proteins necessary for virus transcription and genome replication. An alternative explanation for attenuated virus growth in macrophages is that the diminished levels of VP35, VP40, and supposedly VP24 affect their ability to carry out the innate immune-modulatory functions ascribed to them (Ramanan et al., 2011; Valmas et al., 2010). Therefore, in order to test the latter hypothesis, we measured the expression of selected cytokine and chemokine genes in human macrophages mock-infected or infected with 01Uga07, wt 371Bat, rMbg and rMbg/GFP viruses. In support of this hypothesis, rMbg/GFP virus elicited increased anti-viral inflammatory mediators over levels observed when macrophages were infected with non-GFP MARVs (Fig. 4C). These differences were most striking with CXCL10/IP-10 and CCL5/RANTES, with more modest differences seen for CCL4/MIP-1β and tumor necrosis factor (TNF). Several other cytokines remained unchanged independent of the type of MARV used for infection, including IL6, IL8, IL1RN, IL1β, and IL12β (Fig. 4C and data not shown).

To determine if the extra-cistronic gene insertion between NP and VP35 causes similar downstream mRNA reductions in other filoviruses, a recombinant Ebola virus (rEbov) also containing GFP inserted between NP and VP35 (Towner et al., 2005) was tested using the same assay. As expected, only rEbov with GFP inserted in the NP-VP35 intergenic region elicited detectable cytokine/chemokine responses over the equivalent non-GFP virus (data not shown). The similarity of responses elicited in human macrophages by both MARVs and EBOVs containing an extra-cistronic gene suggests that important immune-modulatory functions can be perturbed when the natural order of transcription is altered by the insertion of an additional transcription unit. Our results are consistent with previous reports describing

the low pathogenicity of GFP-containing EBOVs in infected mice and NHPs (Ebihara et al., 2007).

Conclusions

We report here a reverse genetics system that reliably generates an infectious MARV whose sequence is identical to a virus originally isolated directly from a *R. aegyptiacus* bat (371Bat). We also report the successful rescue of this bat-derived virus containing an insertion of the GFP reporter gene, as well as a robust GFP-based mini-genome reporter system. Although virus rescue systems have been previously developed for MARV (Musoke), such viruses were originally isolated from human clinical samples followed by multiple rounds of virus passage in cell culture (Ebihara et al., 2005; Hoenen et al., 2011). These virus passage histories may have allowed for the accumulation of adaptive mutations detrimental for virus replication in its cognate reservoir host. The full-length genomes reported here have identical sequence to the second VeroE6 passage of the 371Bat isolate, and as such are more authentic tools for examining how MARVs replicate and survive in their zoonotic reservoir.

MARVs containing both GFP and wild type full-length recombinant genomes are rescued with high efficiency and reproducibility. We hypothesize that the use of codon-optimized support plasmids leads to more rapid viral protein production and, when used in a slower-growing but transfectable cell type (BHK-21), the prolonged time-to-death allows for greater numbers of complete virions to be produced for eventual rescue. Based on data from mini-genome studies, it has been previously suggested that insertion of GFP in the NP-VP35 intergenic region may alter the ratio of viral proteins such that virion production suffers and virus rescue may not be possible (Muhlberger et al., 1998; Schmidt et al., 2011). Our results show that reporter genes are well tolerated in this particular region with no adverse effects on infectious virus rescue or growth. However, the insertion of GFP gene between GP-VP40 genes, or after the L gene, seems to be highly detrimental in our system.

Further, and importantly, our data also suggests that such insertions may result in delayed or decreased transcription of viral genes proposed to modulate the immune system, which may explain the higher expression of anti-viral genes and the growth defect of rMbg/GFP observed in human macrophages. We expect that wild type and reporter-containing recombinant marburgviruses based on bat-derived virus isolates will prove invaluable for future studies in the natural reservoir and potential spillover hosts.

Materials and methods

Cell culture and biosafety

All work with infectious Marburg virus and attempts to rescue the virus from cDNA were performed in a biosafety level 4 (BSL-4) facility. BSR-T7/5 cells were a generous gift from K. Conzelmann. BSR-T7/5, BHK21, and VeroE6 cells were propagated in Dulbecco′s modified Eagle′s medium (DMEM) supplemented with 5% fetal bovine serum (FBS) and penicillin-streptomycin as recommended by the manufacturer (Invitrogen). BSR-T7/5 cells

were maintained under G-418 (1 mg/ml Geneticin; Invitrogen) selection pressure every other passage.

Terminal sequences of viral genome

The genomic sequence of the Marburg 371Bat virus isolate (Genbank FJ750958) was previously reported (Towner et al., 2009), but the 5′ and 3′ termini of the RNA corresponded to primer sequences. Viral RNA from this isolate was therefore used as the template to determine the terminal sequences and to generate all cDNA clones. The 5′ and 3′ termini of the virus were determined by rapid amplification of cDNA ends (RACE) using FirstChoice RLM-RACE kit (Ambion) and previously reported protocols (Dodd et al., 2011), respectively.

Plasmid construction

(A) Mini-genome. Two fragments consisting of 103 and 637 nt from the 5′ and 3′ antigenome ends, respectively, were amplified by RT-PCR using the SuperScript III One-Step RT-PCR system with Platinum *Taq* High Fidelity (Invitrogen). These fragments were cloned into a standard T7 transcription vector (Albarino et al., 2009), yielding an empty mini-genome cloned in genomic orientation and flanked by the T7 promoter (5′ terminus) and the hepatitis delta virus ribozyme and T7 polymerase terminator motifs (3′ terminus). The enhanced GFP ORF (GFP) was inserted into the empty mini-genome between the RACE-corrected 103 and 637 nt fragments such that GFP expression is driven by the NP gene transcription start and the L gene transcription termination sequences. **(B) Full-length clones.** Three fragments of similar size spanning the full-length genome of 371Bat Marburg virus were amplified by RT-PCR. Each of these fragments was cloned independently, sequenced to completion, and used to assemble the full-length antigenome into the T7 transcription vector (a detailed cloning strategy is available upon request). The final plasmid contained the full-length antigenome (viral complementary sense) flanked by the T7 RNA polymerase promoter, including an additional 5′ guanine (*G*) which is required for efficient initiation of the T7 RNA polymerase, and followed by hepatitis delta virus ribozyme and T7 polymerase terminator motifs. A spurious nt change (silent mutation) in the *L* gene was kept to differentiate the recombinant virus from the wild type virus. Moreover, the full-length 371Bat Marburg virus genome was cloned into the same T7 transcription plasmid in viral (genome) sense. **(C) GFP-expressing full-length clones.** Three different full-length antigenomic clones were constructed carrying the enhanced GFP ORF (GFP) inserted at position 2849, 8718, or 19037. In all these constructs, the GFP ORF was flanked by 12 and 11nt corresponding to the transcription start and transcription termination of the NP gene, respectively. Similarly, three full-length genomic (viral sense) clones containing identical GFP insertions were cloned into the T7 transcription plasmid. (**D) Support plasmids.** The ORFs encoding Marburg NP, VP35, VP30, and L were amplified by RT-PCR and cloned into the pCAGGS expression plasmid (Niwa et al., 1991) using standard cloning techniques. The T7 RNA polymerase gene was amplified from BL21 bacterial cells and cloned into pCAGGS. Synthetic genes containing codon-optimized NP, VP35, VP30, L, and T7 RNA polymerase ORFs were obtained from a commercial source (GenScript) and cloned into pCAGGS similarly to the wild type ORFs. On average, the synthetic genes are 73–76% identical to the wild type sequences. The resulting plasmids were transformed into XL-10

Gold competent bacterial cells (Stratagene) and purified using standard protocols (Mini- or Maxi-Prep kit; Qiagen). Prior to use, all plasmids were sequenced to completion using standard protocols (BigDye3.1; Applied Biosystems).

Mini-genome expression

BSR-T7/5 cells seeded to approximately 75% confluency in 12-well plates were transfected with 1.5 μg of Marburg mini-genome plasmid, 0.5 μg pC-L, 0.5 μg pC-NP, 0.05 μg pC-VP35, 0.05 μg pC-VP30, and 8 μl LT1 transfection reagent following the manufacturer′s protocol (Mirus Biotech). The four support plasmids were necessary for a single cell to most efficiently replicate and transcribe the GFP mini-genome. GFP expression was determined by direct UV microscopy on live cells.

Rescue of infectious viruses

Viral rescue was attempted in BSRT7/5 cells constitutively expressing the T7 RNA polymerase, and in BHK21 cells that required the addition of a fifth support plasmid, pC-T7, to drive the transcription of the full-length genome. Briefly, a subconfluent (~60–70%) cell monolayer growing in 12-well plates were transfected with 1.5 μg pMbg, 0.5 μg pC-L, 0.5 μg pC-NP, 0.05 μg pC-VP35, 0.05 μg pC-VP30, 0.5 μg of pC-T7 (for BHK21 only), and 10 μl LT1 transfection reagent (Mirus Biotech). Supernatants from the transfected cells were harvested four days post-transfection and clarified by low-speed centrifugation. All rescued viruses were propagated after a 1:5 dilution in DMEM by infecting (~80%) confluent monolayers of VeroE6 cells seeded in T25 flasks. Clarified virus supernatants were then diluted and passed once more to generate a working stock of virus for subsequent experiments. Altogether, the passage history of all viruses used in these studies was one passage in BSR-T7/5 or BHK21 cells and two passages in VeroE6 cells. After the second passage, virus supernatants were inactivated with Tripure (Roche) and RNA extracted using RNeasy kits (Qiagen). The exact molecular identity of each recombinant virus was confirmed by full-genome sequencing following the manufacturer′s protocols (BigDye3.1; Applied Biosystems).

Virus titration and growth curves

All viruses were titrated using a standard 50% tissue culture infective dose (TCID50) protocol in VeroE6 cells. Growth curves were obtained in VeroE6 cells seeded in T25 flasks that were infected at a multiplicity of infection (MOI) of 0.01 with rMbg, rMbg/GFP, or wild type Mbg 371Bat. After a 1 h adsorption, the inoculum was removed, monolayers were washed three times with PBS, and DMEM containing 2% FBS was added to replenish media. The first sample was taken immediately to represent the $t = 0$, and subsequent samples were taken from 1 to 7 days post-infection and stored at −70 °C for subsequent titration by TCID50 assay. For visualization of infected cells, monolayers were fixed (4% formaldehyde in PBS) at four days post-infection and subsequently labeled with a rabbit anti-Marburg polyclonal antibody and anti-rabbit Alexafluor 498 or 594 nm secondary antibodies (Molecular Probes).

Infection of human macrophages

Peripheral blood mononuclear cells were obtained from healthy human donors, and CD14+ cells were purified using magnetically coupled CD14 antibodies (Miltenyi Biotech) as described previously (McElroy and Nichol, 2012). CD14+ cells were grown in 24 well plates in complete media (RPMI with 5% FBS, 100 U/ml of penicillin, 100 μg/ml of streptomycin, and 2 mM L-glutamine) for 7 days to mature to macrophages. To determine the infectivity of wild type and recombinant MARV on CD14+ cells, matured human macrophages were infected with either 01Uga07, 371Bat, rMbg or rMbg/GFP at an MOI of 0.1. Supernatants were collected over five days and titers were obtained on VeroE6 cells using standard TCID50 assay.

To determine the cytokine response of CD14+ cells, matured human macrophages were infected in duplicate at an MOI of 2 with the viruses indicated above. After 1 h adsorption, the inoculum was removed, cells were washed and the media was replenished. At 24 h post-infection, supernatants were collected and cells were lysed for RNA purification.

To standardize extracted RNA, the housekeeping gene GAPDH was measured by qRT-PCR using TaqMan® GAPDH Control Reagents (human) following the manufacturer′s protocol (Applied Biosystems). A customized qRT-PCR array (SABiosciences) was designed to measure the gene expression of 12 inflammatory-related genes (IL1RN, IL1β, IL8, IL6, IL12β, IFNA1, TNF, CCL2, CCL5, CCL4, CCL3, and CXCL10) using SuperScript® III Platinum® SYBR® Green One-Step qRT-PCR Kit and following the manufacturer′s protocols (Invitrogen). Data was calculated from two independent experiments, with mean and standard error of the mean (SEM) calculated from duplicate wells, and plotted as fold induction over mock-infected cells.

Acknowledgments

We thank K. Conzelmann for providing BSRT7/5 cells and Christina Spiropoulou for excellent advice and criticism for this work. Dr. Luke Uebelhoer holds a fellowship supported by the Research Participation Program at the Centers for Disease Control and Prevention (CDC) administered by the Oak Ridge Institute for Science and Education (ORISE) through an interagency agreement between the U.S. Department of Energy (DOE) and CDC.

References

Albarino CG, Bergeron E, Erickson BR, Khristova ML, Rollin PE, Nichol ST. Efficient reverse genetics generation of infectious Junin viruses differing in glycoprotein processing. J. Virol. 2009; 83:5606–5614. [PubMed: 19321606]

Amman BR, Carroll SA, Reed ZD, Sealy TK, Balinandi S, Swanepoel R, Kemp A, Erickson BR, Comer JA, Campbell S, Cannon DL, Khristova ML, Atimnedi P, Paddock CD, Crockett RJ, Flietstra TD, Warfield KL, Unfer R, Katongole-Mbidde E, Downing R, Tappero JW, Zaki SR, Rollin PE, Ksiazek TG, Nichol ST, Towner JS. Seasonal pulses of Marburg virus circulation in juvenile *Rousettus aegyptiacus* bats coincide with periods of increased risk of human infection. PLoS Pathog. 2012; 8:e1002877. [PubMed: 23055920]

Buchholz UJ, Finke S, Conzelmann KK. Generation of bovine respiratory syncytial virus (BRSV) from cDNA: BRSV NS2 is not essential for virus replication in tissue culture, and the human RSV leader region acts as a functional BRSV genome promoter. J. Virol. 1999; 73:251–259. [PubMed: 9847328]

Dodd KA, Bird BH, Khristova ML, Albarino CG, Carroll SA, Comer JA, Erickson BR, Rollin PE, Nichol ST. Ancient ancestry of KFDV and AHFV revealed by complete genome analyses of viruses

isolated from ticks and mammalian hosts. PLoS Negl.Trop. Dis. 2011; 5:e1352. [PubMed: 21991403]

Ebihara H, Groseth A, Neumann G, Kawaoka Y, Feldmann H. The role of reverse genetics systems in studying viral hemorrhagic fevers. Thromb. Haemost. 2005; 94:240–253. [PubMed: 16113812]

Ebihara H, Theriault S, Neumann G, Alimonti JB, Geisbert JB, Hensley LE, Groseth A, Jones SM, Geisbert TW, Kawaoka Y, Feldmann H. In vitro and in vivo characterization of recombinant Ebola viruses expressing enhanced green fluorescent protein. J. Infect. Dis. 2007; 196(Suppl. 2):S313–322. [PubMed: 17940966]

Enterlein S, Volchkov V, Weik M, Kolesnikova L, Volchkova V, Klenk HD, Muhlberger E. Rescue of recombinant Marburg virus from cDNA is dependent on nucleocapsid protein VP30. J. Virol. 2006; 80:1038–1043. [PubMed: 16379005]

Feldmann H, Muhlberger E, Randolf A, Will C, Kiley MP, Sanchez A, Klenk HD. Marburg virus, a filovirus: messenger RNAs, gene order, and regulatory elements of the replication cycle. Virus Res. 1992; 24:1–19. [PubMed: 1626422]

Fritz EA, Geisbert JB, Geisbert TW, Hensley LE, Reed DS. Cellular immune response to Marburg virus infection in cynomolgus macaques. Viral Immunol. 2008; 21:355–363. [PubMed: 18788943]

Geisbert TW, Jaax NK. Marburg hemorrhagic fever: report of a case studied by immunohistochemistry and electron microscopy. Ultrastructural Pathol. 1998; 22:3–17.

Hensley LE, Alves DA, Geisbert JB, Fritz EA, Reed C, Larsen T, Geisbert TW. Pathogenesis of Marburg hemorrhagic fever in cynomolgus macaques. J. Infect. Dis. 2011; 204(Suppl. 3):S1021–1031. [PubMed: 21987738]

Hoenen T, Groseth A, de Kok-Mercado F, Kuhn JH, Wahl-Jensen V. Minigenomes, transcription and replication competent virus-like particles and beyond: reverse genetics systems for filoviruses and other negative stranded hemorrhagic fever viruses. Antiviral Res. 2011; 91:195–208. [PubMed: 21699921]

McElroy AK, Nichol ST. Rift Valley fever virus inhibits a pro-inflammatory response in experimentally infected human monocyte derived macrophages and a pro-inflammatory cytokine response may be associated with patient survival during natural infection. Virology. 2012; 422:6–12. [PubMed: 22018491]

Muhlberger E, Lotfering B, Klenk HD, Becker S. Three of the four nucleocapsid proteins of Marburg virus, NP, VP35, and L, are sufficient to mediate replication and transcription of Marburg virus-specific monocistronic minigenomes. J. Virol. 1998; 72:8756–8764. [PubMed: 9765419]

Muhlberger E, Weik M, Volchkov VE, Klenk HD, Becker S. Comparison of the transcription and replication strategies of marburg virus and Ebola virus by using artificial replication systems. J. Virol. 1999; 73:2333–2342. [PubMed: 9971816]

Neumann G, Feldmann H, Watanabe S, Lukashevich I, Kawaoka Y. Reverse genetics demonstrates that proteolytic processing of the Ebola virus glycoprotein is not essential for replication in cell culture. J. Virol. 2002; 76:406–410. [PubMed: 11739705]

Niwa H, Yamamura K, Miyazaki J. Efficient selection for high-expression transfectants with a novel eukaryotic vector. Gene. 1991; 108:193–199. [PubMed: 1660837]

Paweska JT, Jansen van Vuren P, Masumu J, Leman PA, Grobbelaar AA, Birkhead M, Clift S, Swanepoel R, Kemp A. Virological and serological findings in Rousettus aegyptiacus experimentally inoculated with vero cells-adapted hogan strain of Marburg virus. PLoS One. 2012; 7:e45479. [PubMed: 23029039]

Ramanan P, Shabman RS, Brown CS, Amarasinghe GK, Basler CF, Leung DW. Filoviral immune evasion mechanisms. Viruses. 2011; 3:1634–1649. [PubMed: 21994800]

Sanchez, A., Geisbert, TW., Feldmann, H. Filoviridae: Marburg and Ebola viruses. In: Knipe, DMaH, P, M., editors. Fields Virology. fifth. Lippincott, Williams and Wilkins; Philadelphia: 2007. p. 1410-1448.

Schmidt KM, Schumann M, Olejnik J, Krahling V, Muhlberger E. Recombinant Marburg virus expressing EGFP allows rapid screening of virus growth and real-time visualization of virus spread. J. Infect. Dis. 2011; 204(Suppl. 3):S861–870. [PubMed: 21987762]

Swanepoel R, Smit SB, Rollin PE, Formenty P, Leman PA, Kemp A, Burt FJ, Grobbelaar AA, Croft J, Bausch DG, Zeller H, Leirs H, Braack LE, Libande ML, Zaki S, Nichol ST, Ksiazek TG, Paweska

JT. Studies of reservoir hosts for Marburg virus. Emerg. Infect. Dis. 2007; 13:1847–1851. [PubMed: 18258034]

Tamura K, Peterson D, Peterson N, Stecher G, Nei M, Kumar S. MEGA5: molecular evolutionary genetics analysis using maximum likelihood, evolutionary distance, and maximum parsimony methods. Mol. Biol. Evol. 2011; 28:2731–2739. [PubMed: 21546353]

Towner JS, Amman BR, Sealy TK, Carroll SA, Comer JA, Kemp A, Swanepoel R, Paddock CD, Balinandi S, Khristova ML, Formenty PB, Albarino CG, Miller DM, Reed ZD, Kayiwa JT, Mills JN, Cannon DL, Greer PW, Byaruhanga E, Farnon EC, Atimnedi P, Okware S, Katongole-Mbidde E, Downing R, Tappero JW, Zaki SR, Ksiazek TG, Nichol ST, Rollin PE. Isolation of genetically diverse Marburg viruses from Egyptian fruit bats. PLoS Pathog. 2009; 5:e1000536. [PubMed: 19649327]

Towner JS, Paragas J, Dover JE, Gupta M, Goldsmith CS, Huggins JW, Nichol ST. Generation of eGFP expressing recombinant Zaire ebolavirus for analysis of early pathogenesis events and high-throughput antiviral drug screening. Virology. 2005; 332:20–27. [PubMed: 15661137]

Towner JS, Pourrut X, Albarino CG, Nkogue CN, Bird BH, Grard G, Ksiazek TG, Gonzalez JP, Nichol ST, Leroy EM. Marburg virus infection detected in a common African bat. PLoS One. 2007; 2:e764. [PubMed: 17712412]

Valmas C, Grosch MN, Schumann M, Olejnik J, Martinez O, Best SM, Krahling V, Basler CF, Muhlberger E. Marburg virus evades interferon responses by a mechanism distinct from ebola virus. PLoS Pathog. 2010; 6:e1000721. [PubMed: 20084112]

Volchkov VE, Volchkova VA, Muhlberger E, Kolesnikova LV, Weik M, Dolnik O, Klenk HD. Recovery of infectious Ebola virus from complementary DNA: RNA editing of the GP gene and viral cytotoxicity. Science. 2001; 291:1965–1969. [PubMed: 11239157]

A

		1	2	3	4	5	6	7	8
1.MARV 371batUga2007	(B)								
2.MARV 01Uga2007	(H)	99							
3.MARV Musoke-Ken1980	(H)	93	93						
4.MARV 01Uga-Net2008	(H)	92	92	94					
5.MARV 164ObatUga2008	(B)	92	92	94	98				
6.RAVN Rav-Ken1987	(H)	79	79	79	79	79			
7.RAVN 1304ObatUga2009	(B)	79	79	79	79	79	99		
8.RAVN 02Uga2007	(H)	79	79	79	79	79	99	99	

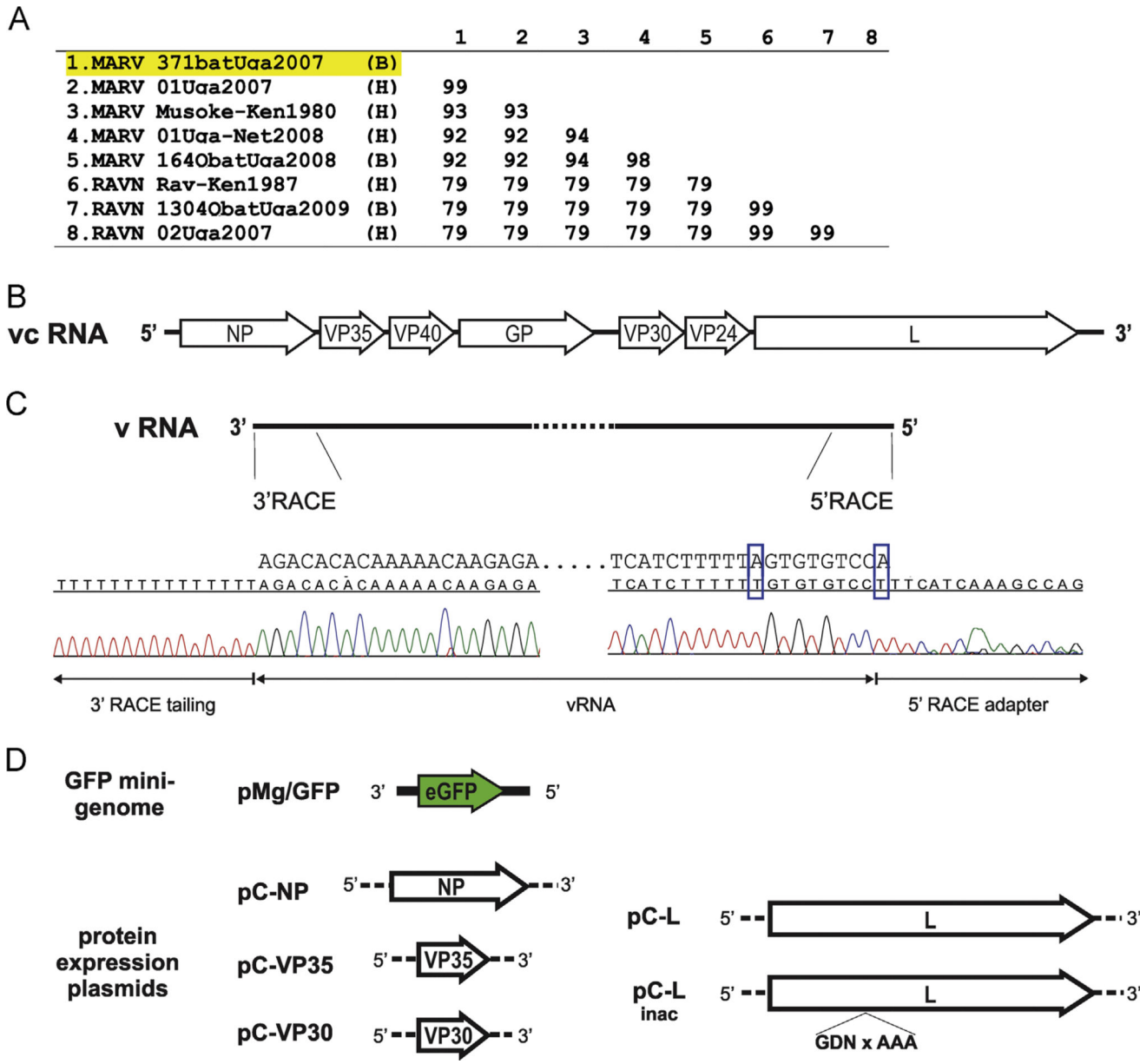

Fig. 1.

(A) Sequence similarity of Marburg virus 371Bat isolate to other known bat (*B*) and human (*H*) isolates. Sequences obtained from Genbank (FJ750958, FJ750957, DQ217792, JN408064, JX458853, DQ447649, JX458857, FJ750953) were aligned and the nucleotide similarity was determined using Mega5 (Tamura et al., 2011). (B) Basic organization of the marburgvirus genome. The seven ORFs are depicted in the viral complementary sense (5′ to 3′). (C) 5′ and 3′ terminal sequences currently reported for 371Bat isolate (top, Genbank #FJ750958) compared to sequencing results of 371Bat isolate obtained by RACE (bottom). Chromatograms are displayed below sequences, and blue boxes indicate where RACE sequence diverges from reported sequence. (D) Schematic of GFP mini-genome plasmid with 371Bat 5′ and 3′ UTRs (black line), and viral protein expression plasmids used in

both mini- and full-length genome experiments (dashed line indicates pCAGGS plasmid sequence).

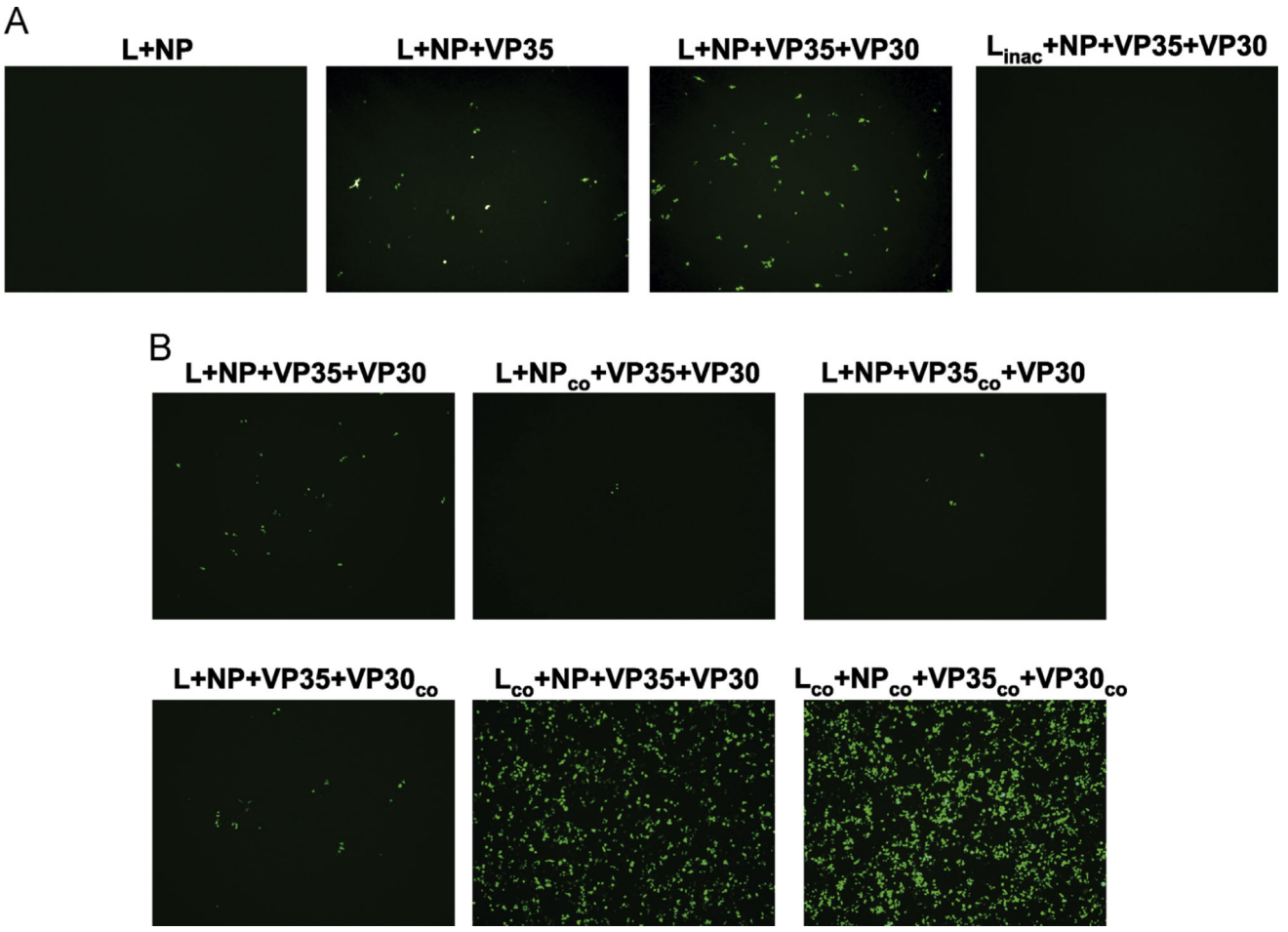

Fig. 2.

Replication of 371Bat-based GFP mini-genome. GFP expression was assessed as an indicator of mini-genome replication in BSR-T7/5 cells using (A) wild type and (B) codon-optimized viral protein support plasmids. Images were taken either four days (A) or two days (B) post-transfection.

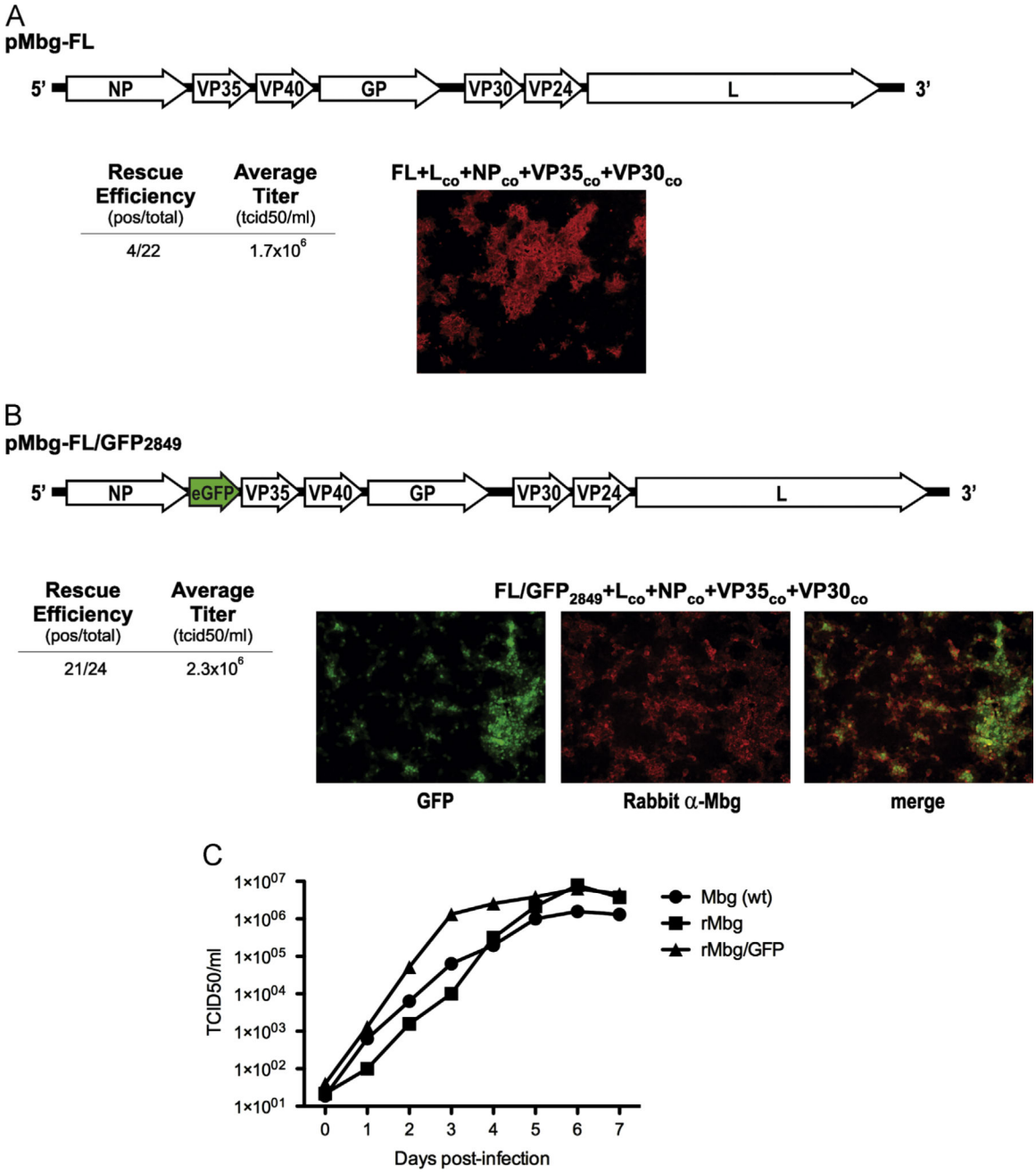

Fig. 3.

Rescue and characterization of recombinant 371Bat MARV using full-length viral complementary genomes. (A) Wild type recombinant MARV (rMbg) was rescued in BHK-21 cells using the full-length genome depicted, T7 polymerase plasmid, and codon-optimized viral support protein plasmids NP, VP35, VP30, and L. Efficiency of rescue in a single experiment is shown as wells positive/total wells, and average titer was assessed by standard TCID50 assay. VeroE6 cells were infected with rMbg virus, fixed 4 days post-infection, and stained for immunofluoresence assay (IFA) using a polyclonal rabbit anti-Marburg antibody followed by anti-rabbit Alexa-Fluor 594. (B) A recombinant MARV

containing the GFP ORF in the intergenic region of NP and VP35 (rMbg/GFP) was rescued under similar conditions as wild type. VeroE6 cells were infected with rMbg/GFP virus and visualized for GFP expression (left) or subjected to the same immunofluorescence assay as in (A) (middle, merged images at right). (C) Wild type 371Bat (Mbg (wt)), rMbg, and rMbg/GFP viruses were used to infect VeroE6 cells at an MOI of 0.01 to assess growth kinetics. Adsorption was allowed for 1 h, after which cells were washed with PBS and given complete growth media. At time points indicated, supernatant was taken and titered by TCID50 assay on VeroE6 cells.

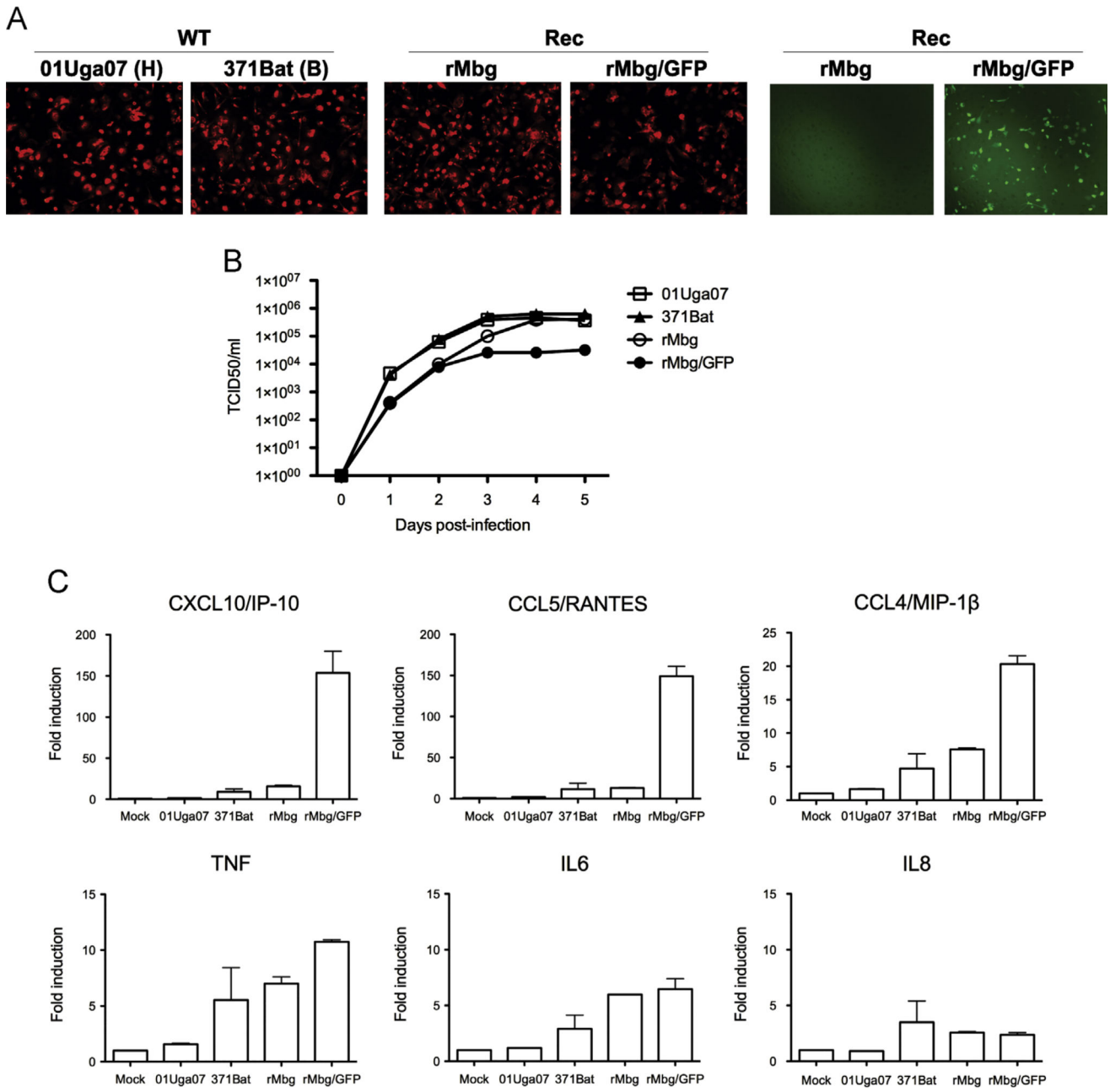

Fig. 4.

(A) Infection of human macrophages with wild type or recombinant MARV. CD14+ monocytes were allowed to mature to macrophages for 7 days and infected with indicated viruses at an MOI of 0.1. IFA was performed as in Fig. 3. (B) Growth kinetics of wild type or recombinant MARV in CD14+ macrophages. Titers were obtained on VeroE6 cells as in Fig. 3C. (C) Pro-inflammatory responses of human macrophages infected with wild type or recombinant marburgviruses. Seven days post-maturation, cells were infected with the indicated viruses at an MOI of 2 and total RNA was harvested 24 h later. Expression of

inflammatory-related genes was assessed using a custom qRT-PCR array, and plotted as fold induction over mock-infected cells.